JOURNAL OF GEOPHYSICAL RESEARCH, VOL. 113, C07023, doi:10.1029/2007JC004644, 2008

Tidal and spring-neap variations in horizontal dispersion in a partially mixed estuary

W. R. Geyer,[1] R. Chant,[1] and R. Houghton[1]

Received 14 November 2007; revised 25 February 2008; accepted 21 March 2008; published 18 July 2008.

[1] A sequence of dye releases in the Hudson River estuary provide a quantitative assessment of horizontal dispersion in a partially mixed estuary. Dye was released in the bottom boundary layer on 4 separate occasions, with varying tidal phase and spring-neap conditions. The three-dimensional distribution of dye was monitored by two vessels with in situ, profiling fluorometers. The three-dimensional spreading of the dye was estimated by calculating the time derivative of the second moment of the dye in the along-estuary, cross-estuary and vertical directions. The average along-estuary dispersion rate was about 100 m^2/s, but maximum rates up to 700 m^2/s occurred during ebb tides, and minimum rates occurred during flood. Vertical shear dispersion was the principal mechanism during neap tides, but transverse shear dispersion became more important during springs. Suppression of mixing across the pycnocline limited the vertical extent of the patch in all but the maximum spring-tide conditions, with vertical diffusivities in the pycnocline estimated at 4×10^{-5} m^2/s during neaps. The limited vertical extent of the dye patch limited the dispersion of the dye relative to the overall estuarine dispersion rate, which was an order of magnitude greater than that of the dye. This study indicates that the effective dispersion of waterborne material in an estuary depends sensitively on its vertical distribution as well as the phase of the spring-neap cycle.

Citation: Geyer, W. R., R. Chant, and R. Houghton (2008), Tidal and spring-neap variations in horizontal dispersion in a partially mixed estuary, *J. Geophys. Res.*, *113*, C07023, doi:10.1029/2007JC004644.

1. Introduction

[2] *Taylor* [1954] demonstrated that the horizontal spreading of waterborne material is greatly enhanced by the combination of vertical shear and vertical mixing. His famous equation for horizontal shear dispersion K_x is

$$K_x = \alpha \frac{u^2 h^2}{K_{zo}} \tag{1}$$

where u is a representative velocity, h is the water depth, K_{zo} is a representative value of the vertical turbulent diffusivity K_z, and α is a coefficient ($\sim 1-10 \times 10^{-3}$) that depends on the vertical structure of the velocity and diffusivity, as

$$\alpha = \int \tilde{u} \int \frac{1}{\tilde{k}} \int \tilde{u} d\varsigma'' d\varsigma' d\varsigma \tag{2}$$

[*Bowden*, 1965], where ς is a nondimensional vertical coordinate, and $\tilde{u}$ and $\tilde{k}$ are nondimensional structure functions for the velocity and vertical diffusivity, respectively. Taylor's equation has the paradoxical result that shear dispersion varies inversely with the rate of vertical mixing. Many authors have revisited this problem for various applications, one of the most notable being estuarine dispersion [*Bowden*, 1965; *Okubo*, 1973; *Smith*, 1977]. *Bowden* [1965] estimates that $K_x = 170$ m^2/s in the Mersey estuary based on the contributions of the vertical shear and mixing. He also noted that the overall dispersion was about a factor of 2 larger, due to lateral variations. The contribution of lateral variations to shear dispersion was taken up by *Fischer* [1972] (also see *Fischer et al.* [1979]).

[3] There are a number of circumstances that can alter the dispersion rate, notably time-dependence [*Fischer et al.*, 1979; *Young and Rhines*, 1982], incomplete vertical or lateral mixing [*Bowden*, 1965; *Okubo*, 1973], and lateral shear [*Fischer*, 1972; *Sumer and Fischer*, 1977]. In most estuaries, the oscillatory shear due to the tides is significantly larger than the mean shear due to the estuarine circulation, and so the dispersion may be dominated by the tidal processes. Whether or not tidal dispersion dominates depends on the timescale of vertical mixing relative to the tidal period $K_z T/h^2$, where T is the tidal period [*Young and Rhines*, 1982; *Fischer et al.*, 1979]. For values of this parameter much less than 1 (e.g., $K_z < 10^{-3}$ m^2/s for a 10-m deep estuary), tidal dispersion is limited due to incomplete vertical mixing, so the shear dispersion due to the mean, estuarine shear may be more important even though its amplitude is significantly less than the tidal shear.

[4] The dispersion process is further complicated by the tidal variation in vertical mixing rate due to tidal straining

[1]Woods Hole Oceanographic Institution, Applied Ocean Physics and Engineering, Woods Hole, Massachusetts, USA.

0148-0227/08/2007JC004644$09.00

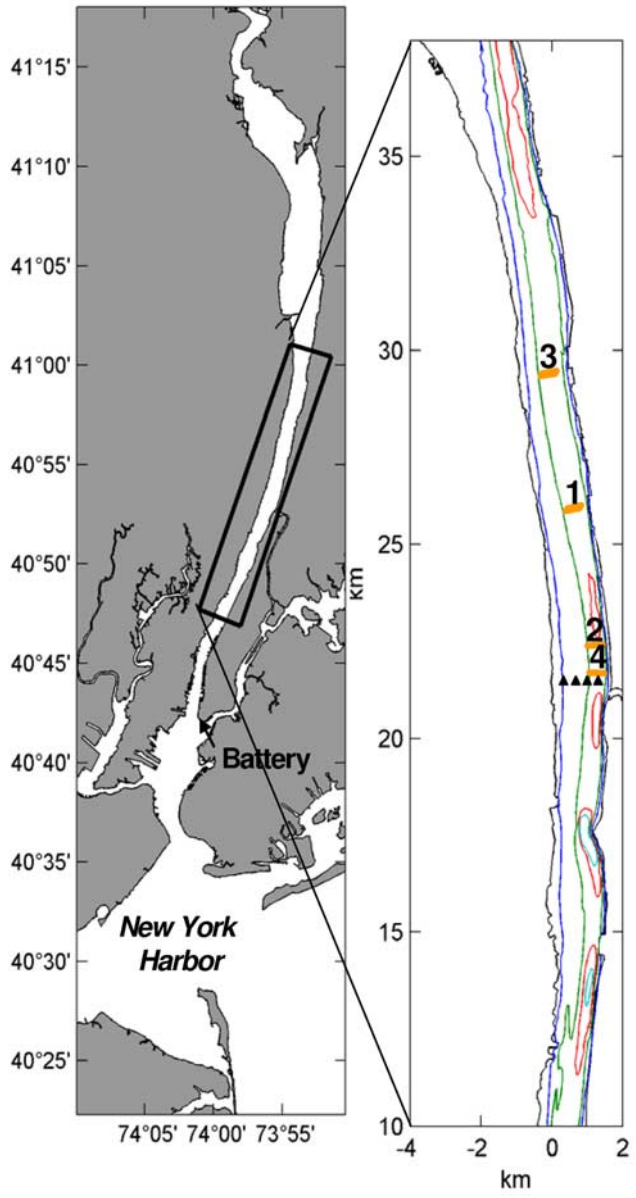

Figure 1. Location map of the study area. The inset shows the locations of the four releases as well as the array of bottom-mounted ADCPs. Isobaths are also shown, with contours of 5, 10, 15, and 20 m depth.

[*Simpson et al.*, 1990; *Jay and Smith*, 1990], which in turn results in tidal variations in the strength of the vertical shear. During the flood, tidal straining reduces the stratification, resulting in enhanced vertical mixing and reduced shear, whereas restratification during the ebb causes reduced mixing and enhanced vertical shear. These variations in shear and mixing rates should lead to large variations in dispersion rate between flood and ebb, with much greater dispersion expected during the ebb. However, depending on the mixing rate, the straining on ebb may not lead to net dispersion.

[5] The effective dispersion rate can be estimated based on the tidally averaged salt balance, in which the net contributions of mean and oscillatory dispersion processes are lumped into a single dispersion coefficient that balances the seaward advection of salt due to freshwater flow:

$$K_{x\,obs} = \frac{u_f s_o}{\partial s/\partial x} \tag{3}$$

where u_f is the freshwater outflow velocity, s_o is a representative value of salinity in the estuary, and $\partial s/\partial x$ is the average along-estuary salinity gradient. Estimates of K_{xobs} are highly variable, but they sometimes reach 10^3 m^2/s or more in stratified estuaries [*Fischer et al.*, 1979; *Monismith et al.*, 2002; *Bowen and Geyer*, 2003; *Banas et al.*, 2004]. This value far exceeds the possible contribution of oscillatory shear dispersion. On the basis of Taylor's formulation of equation (1), the effective vertical mixing rate must be very low, on the order of 10^{-4} m^2/s. This low a rate is not out of the question; even smaller values have been found to reproduce observed estuarine circulation regimes [*Wang and Kravitz*, 1980]. However, such weak vertical mixing rates result in very long timescales for vertical mixing, on the order of tens of days. A very long timescale of vertical mixing means that a tracer is not likely to be distributed uniformly in the vertical direction, which brings into question the validity of a one-dimensional representation of the dispersion process. Indeed, *Bowden* [1965] suggests that the shear dispersion paradigm should only be applied to weakly stratified estuaries (i.e., those with vertical salinity differences exceeding 1 psu). Yet it is only as stratification becomes stronger that the very high effective dispersion rates are observed.

[6] This paper provides a quantitative investigation of horizontal dispersion in a stratified estuary. It adds to a relatively small number of scientific investigations of estuarine dispersion by direct observations of tracer spreading [*Wilson and Okubo*, 1978; *Guymer and West*, 1988; *Tyler*, 1984; *Vallino and Hopkinson*, 1998; *Clark et al.*, 1996]. This study differs from previous studies in that the three-dimensional evolution of the patch was recorded on timescales short enough to resolve the influence of tidal variations of the flow on vertical mixing and horizontal spreading. The release was performed in the Hudson River estuary during moderate discharge conditions and different phases of the spring-neap cycle that included strongly stratified and partially mixed conditions.

2. Methods

[7] The dye study was conducted in the Hudson River estuary (Figure 1) during the spring of 2002. An array of moorings and bottom tripods was deployed across the estuary to measure currents and water properties through the course of the study [*Lerczak et al.*, 2006]. Four dye injections were performed, the first two during neap tides, the third in the transition from neaps to springs, and the fourth during spring tides (Table 1). The releases occurred during a variety of different tidal phases, as indicated in Table 1. River discharge was about 500 m^3/s, which is close to the annual average, although there were discharge events before the first dye release and between the second and third releases, producing stronger horizontal and vertical salinity gradients than average [see *Lerczak et al.*, 2006].

Table 1. Conditions During Dye Releases

Release	Date	Tidal Current Amplitude (near-bottom)	Stratification (Δs, Bottom to Surface)	Phase of Tide During Release
1	May 5–7	0.6 m/s	16	early ebb
2	May 9–10	0.7	15→13[a]	mid flood
3	May 23–24	0.8	13→8[a]	early ebb
4	May 25–26	0.9	5	early flood

[a]During these releases, the stratification decreased as indicated.

[8] Fluoroscein dye was selected for this study, because it has similar detection limits to Rhodamine, but it is approximately 5 times less expensive, allowing a much larger signal for a given cost. The disadvantage of fluoroscein is that it has a rapid photo-decay rate, with an e-folding timescale of 6–8 hours in near-surface waters [*Smart and Laidlaw*, 1977; J. Ledwell, personal communication, 2007]. A surface release of fluoroscein would be significantly compromised by the nonconservative effect of photo-decay. However, the Hudson estuary is so turbid that the 1% light level occurs between 2 and 3-m depth [*Cole et al.*, 1992], so significant photo-decay would only occur if the dye reached the upper 2 meters of the water column. In order to minimize the problem of photo-decay, only near-bottom dye releases were performed.

[9] Approximately 44 kg of fluoroscein dye was injected near the bottom during each release. The dye was diluted with seawater and alcohol to match the density of the target depth. The diluted dye was pumped through a hose to the target depth, 2–3 m above the bottom. The injection technique produced an initial stripe of dye approximately 1 m thick in the vertical, several m wide, and about 300 m long in the cross-estuary direction. The dye injection took approximately 15 minutes. A CTD (conductivity, temperature, depth recorder) was mounted on the dye injection unit, and the depth of the release was adjusted to maintain nearly constant salinity (and density) throughout the initial patch. In each case, the dye injection took place below the pycnocline and 2–3 m above the bottom.

[10] Two vessels were involved in the dye releases and subsequent surveying. Both vessels were equipped with CTDs that included Chelsea fluorometers, with filters that optimize their detection of fluoroscein. Calibration of these sensors was performed before the field study, using the ambient water from the Hudson, to minimize the influence of background fluorescence on the estimates of dye concentration.

[11] One of the vessels conducted "tow-yo" surveys to obtain high resolution of the dye in the along-estuary direction during the initial spreading of the dye, and in the lateral direction in subsequent surveys. The other vessel performed vertical profiles, mostly on along-estuary transects. The surveys were designed to resolve the three-dimensional distribution of dye during the first 12–18 hours after the release. On subsequent days, after the dye had spread laterally across the estuary, the surveys concentrated on the along-estuary dye distribution.

[12] The dilution and spreading of the dye for the four releases was quantified based on analysis of the transverse survey data, interpolated onto a uniform grid. This gridding process was performed to minimize sampling bias associated with nonuniform spatial sampling of the patch. The gridding was performed for each patch survey, extending over 1–2 hours and including 4–11 transverse lines. The along-estuary position of each of the transverse lines was "advected" to the mean time of the survey, based on observations of the currents measured at a bottom-mounted ADCP in the center of the dye surveying area (Figure 1), averaged from 0.5–5 m above bottom. The corrected along-estuary position was thus determined as $y_a = y_o - \bar{v}(t_o - t_c)$ where y_a is the advected position, y_o is the observed position, $\bar{v}$ is the estimated along-estuary velocity, t_o is the time of the observation, and t_c is the time of the observation at the center of the patch. (Note that for the remainder of the paper, the y-coordinate is designated as the along-channel coordinate, with positive values indicating the up-estuary direction). This advection calculation had a significant influence on both the estimated mass of the dye and on its along-estuary moment. The grid was selected to slightly oversample the measurements (20 grid cells across the estuary and 10 in the along-estuary direction).

[13] The estimated dye inventories were relatively consistent between surveys and between releases (Table 2), although the total mass of dye was underestimated by almost 40% on average [as also noted by *Chant et al.*, 2007]. From the standpoint of quantifying dispersion, it is important to assess whether this discrepancy is due to a systematic calibration problem or to incomplete surveying of the dye patch. The consistency of the mass estimates over a wide range of dispersion conditions is more suggestive of a calibration issue, although the exact cause of the error was not determined.

[14] The contributions of spreading of the dye in the three different dimensions were determined by calculating the 2nd moments of the dye patches, based on the gridded data. The 2nd moment in the vertical was determined at each of the observation points as

$$z'^2 = \frac{\int_0^h z^2 c(z)dz}{\int_0^h c(z)dz} - \bar{z}^2 \tag{4}$$

$\bar{z}$ is the 1st moment of the dye in the vertical. The quantity z' was then gridded along with the dye concen-

Table 2. Dye Mass Estimates (Including Standard Deviation)

Release	Number of Surveys	Estimated Mass, kg
1	6	26 ± 2
2	5	32 ± 4
3	5	23 ± 6
4	3	27 ± 4

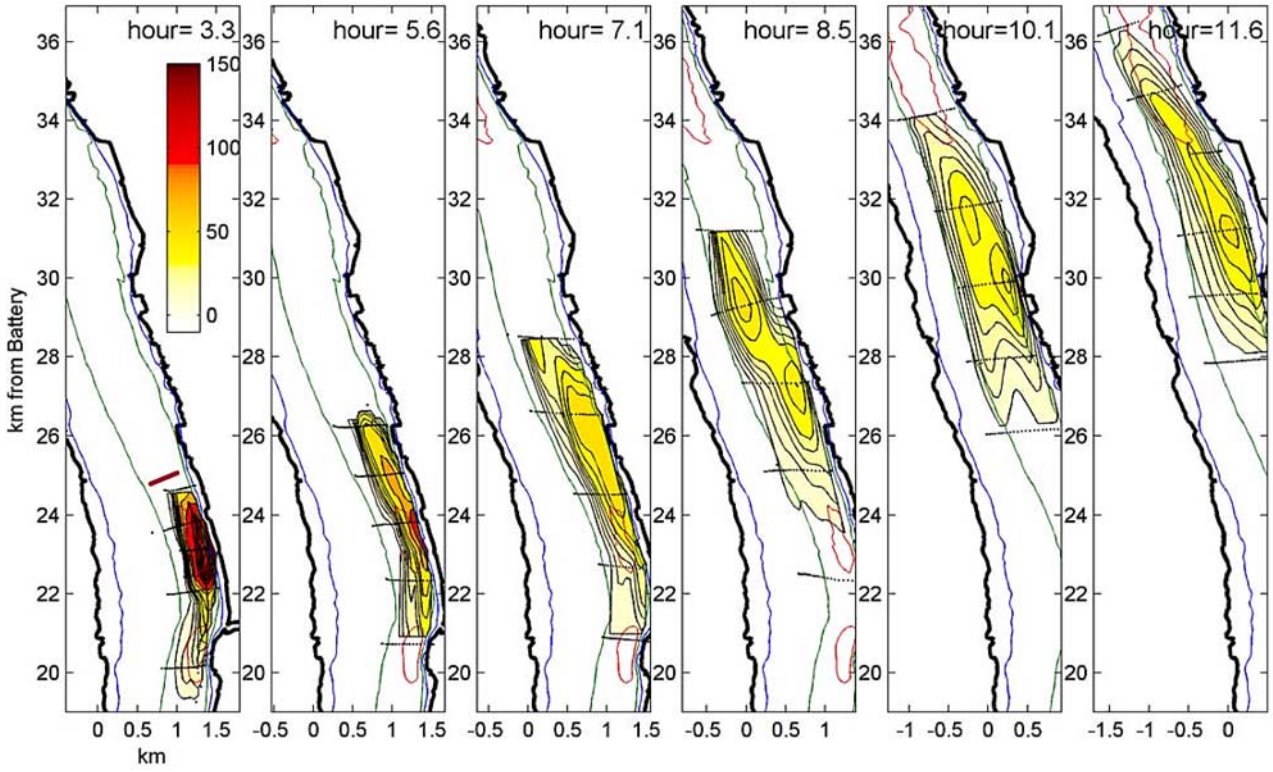

Figure 2. Contours of vertically averaged dye concentration for a sequence of patch surveys during the flood tide following the first release. Concentrations are in units of 10^{-8} kg/m^3. The injection location is shown in red on the left. Hours correspond to time after release. Dots indicate the measurement points. Note that the aspect ratio is distorted by a factor of 2 to provide more detail in the lateral direction. This accentuates the apparent curvature of the domain.

tration (as described above), and the estimate of the vertical moment of the dye was determined by a weighted average of z', i.e.,

$$z'^2_{mean} = \frac{\int\int z'^2 C(x,y)dxdy}{\int\int C(x,y)dxdy} \tag{5}$$

where $C(x, y)$ is the vertical integral of the dye concentration. The second moment in the cross-estuary direction x'^2 was computed from the gridded, vertically integrated concentration data $C(x, y)$ analogously to z'^2_{mean}, where the weighted average is based on the cross-sectionally integrated dye distribution. The second moment in the along-estuary direction was determined by laterally integrating the gridded data and fitting a Gaussian of the form

$$C = C_o \exp\frac{(y-\bar{y})^2}{2y'^2} \tag{6}$$

[15] The value of the second moment y'^2 was determined by a nonlinear least squares fit of the laterally integrated data. Finally, the dispersion rate for each dimension is determined by the time rate of change of the 2nd moment in that direction [e.g., *Fischer et al.*, 1979; *Ledwell et al.*, 1993]

$$K_x = \frac{1}{2}\frac{d}{dt}x'^2 \quad K_y = \frac{1}{2}\frac{d}{dt}y'^2 \quad K_z = \frac{1}{2}\frac{d}{dt}z'^2 \tag{7}$$

3. Results

3.1. Observations of Dye Distributions

[16] The first injection was conducted at km 25 in a 300 m stripe oriented across the estuary in the deeper, east side of the estuary. (Figure 1). The dye was approximately 2-m above the bottom during the injection, in water of salinity 17.5 psu. The dye rapidly mixed to the bottom due to boundary layer turbulence. During the remainder of the ebb, the dye slowly advected southward along the east side of the estuary, with most of the dye remaining in a concentrated patch in the bottom boundary layer, 2-km south of the release point (Figure 2, 1st panel). During the subsequent flood, the patch was advected northward as it spread laterally and vertically (Figure 2). A modest rate of horizontal dispersion is evident in the elongation of the patch.

[17] Along-estuary vertical sections obtained during the flood (Figure 3) indicate that the dye remained within the bottom boundary layer, growing in vertical thickness in measure with the growth of the bottom mixed layer. The

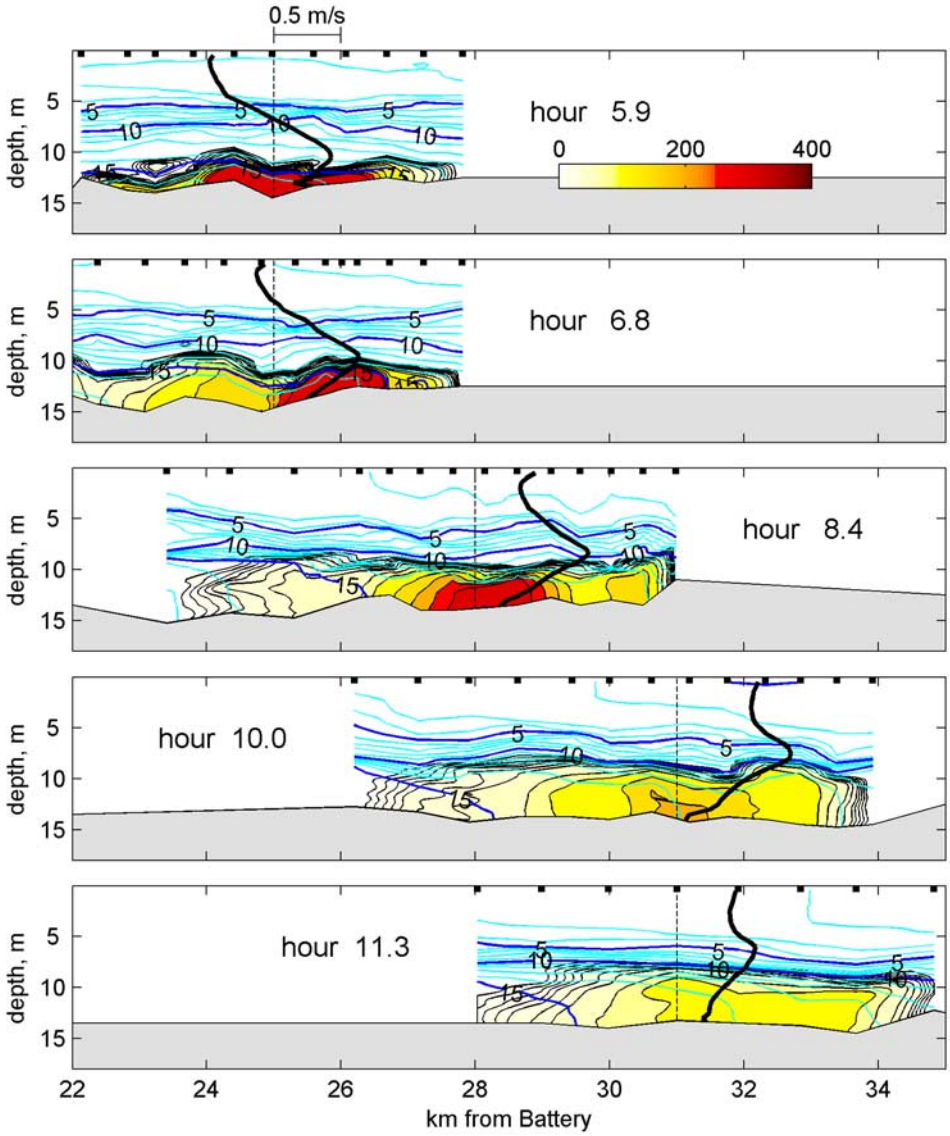

Figure 3. Along-estuary sections of the dye patches during the flood tide following the first release, obtained by the N-S survey vessel. Dye concentration is indicated by the yellow-to-red color contours; salinity is shown in blue line contours. Measurement locations are shown as tics at the surface. Velocity profiles obtained in the middle of each survey by a ship-mounted ADCP are shown in black, with a velocity scale on the uppermost panel. Time after release is indicated.

patch was 2-m thick at the beginning of the flood, and it increased to 6-m by the end. During the flood, dilution of the patch reduced the dye concentrations by nearly an order of magnitude. The dilution of dye was accompanied by a reduction of salinity of the dye, most notably between 6.7 and 8.4 hours, when the dye-weighted salinity dropped from 16.1 to 14.7 psu. This reduction in salinity indicates entrainment of pycnocline water into the bottom boundary layer [*Chant et al.*, 2007], which both diluted the dye and reduced its salinity.

[18] The velocity profiles (indicated in black in Figure 3) indicate strong shears across the boundary layer throughout the flood. A distinct velocity maximum occurred within the pycnocline, due to the superposition of the boundary layer structure with the estuarine shear flow [*Geyer and Farmer*, 1989]. Note that the shear resulted in some straining of the patch (higher concentrations at the top of the leading edge, and at the bottom of the trailing edge) at the end of the flood, although vertical mixing minimized the "tilting" of the dye. The salinity field was also strained by the shear [*Simpson et al.*, 1990] but did not show any evidence of overturning. This difference in the behavior of salt and dye can be explained in that the ratio of horizontal to vertical gradient was more than an order of magnitude larger for dye than for salt. The relative strength of straining to vertical mixing was thus much greater for dye, leading to the inverted dye profile.

[19] The lateral spreading of the dye appeared to be constrained by the geometry of the channel, as indicated by the lateral sections at various times following the first

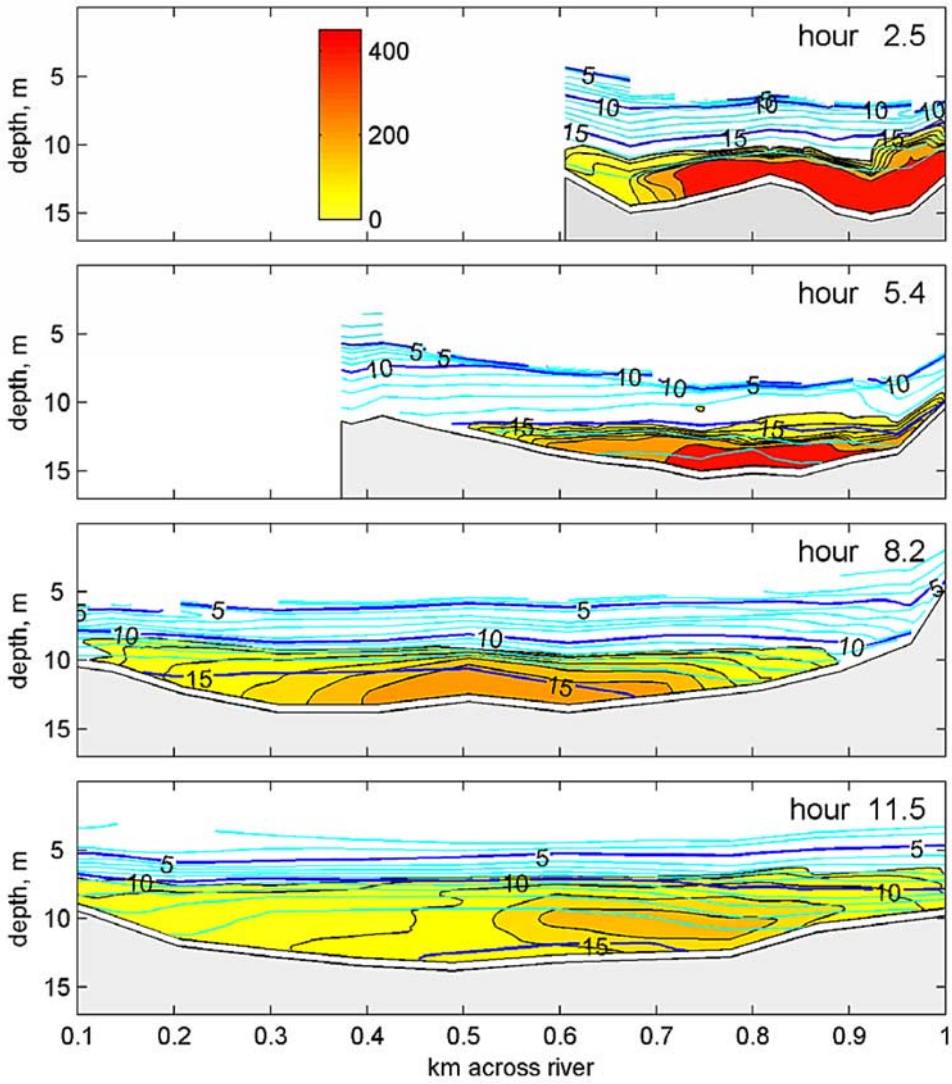

Figure 4. Cross-sections across the estuary at various times following the 1st release. Dye and salinity contours are shown as in Figure 3. Each cross-section is roughly in the center of the patch.

release (Figure 4). The dye was initially confined to a 300-m wide deep section on the east side of the estuary (top panel), and as the geometry of the channel changed and the dye spread vertically, the dye occupied more and more of the width of the estuary. By the end of the flood (11.5 hours after the release), the dye had spread entirely across the estuary. For the most part the lateral gradients of dye followed the isopycnals, which were relatively flat. This distribution indicates that the lateral dispersion was rapid enough that after 1 tidal cycle, the lateral extent of the dye was geometrically constrained, rather than being limited by the lateral dispersion rate. Channel curvature is slight in this reach of the estuary, and it did not appear to have a significant influence on the lateral dye distribution.

[20] The dye patch was tracked for 3 d following the release, although 12-h gaps occurred during nighttime hours. The patch was advected up and down estuary approximately 10-km by the tidal excursion, but there was also a net landward advection of the dye, with a corresponding decrease of the dye-weighted salinity. These processes are consistent with the influence of the estuarine circulation combined with net entrainment of overlying water [*Chant et al.*, 2007].

[21] The second dye release was conducted during similar tidal and stratification conditions as the first, but the release occurred during the flood tide rather than the ebb. The initial spread of the dye was similar to the flood-tide conditions of release 1, with the dye mainly confined to a horizontally compact blob within the relatively well-mixed bottom boundary layer. The distribution during the ebb was very different, however (Figure 5a). The strong vertical shear during the ebb strained the patch of dye, and greatly increased its along-estuary dimension. Note that the straining also caused the lower layer to restratify, reducing the vertical mixing of dye. The tongue-like vertical structure of the dye during the ebb is indicative of the weak vertical mixing during this phase of the tide.

[22] The third release was conducted during conditions intermediate between neap and spring (Table 1), on the same phase of the tide as the 1st release. The dye distribu-

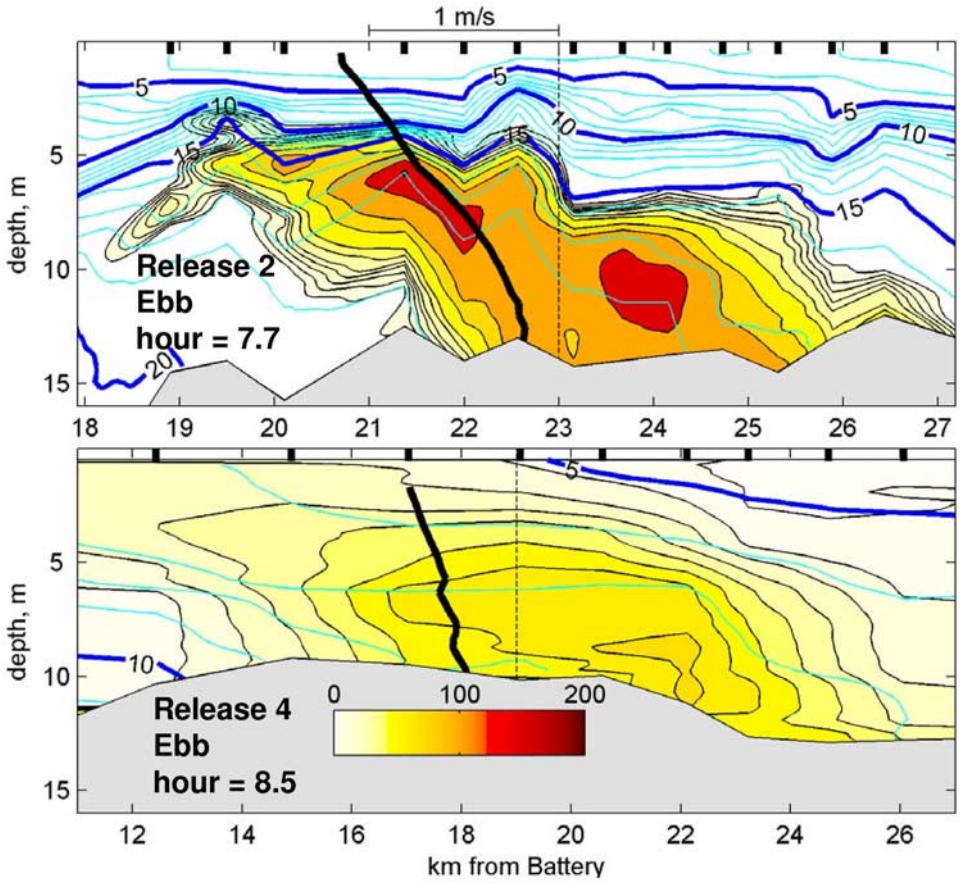

Figure 5. Along-estuary contours of dye and salinity (as in Figure 2) for the ebb phase of the tide during release 2 (top) and release 4 (bottom). Velocity profiles for the middle of the patch are shown in black.

tions were similar to the first release, with increased vertical scales associated with higher mixing rates (quantified in the next section). The 4th release was conducted during spring tide conditions (Table 1 and Figure 5b), with much less salt stratification and significantly increased vertical mixing. The dye was rapidly mixed in the vertical, as evident in the cross-section.

3.2. Quantification of Dilution and Spreading

[23] The dilution of the dye through the course of each release was estimated by calculating the mean concentration of dye from the gridded data for each ''patch'' survey. The definition of ''mean concentration'' for a localized patch depends on the area included in the average. To obtain a consistent estimate of dilution, a threshold concentration of 5% of the observed maximum for the patch was selected. This is equivalent to the 2nd standard deviation of a Gaussian distribution.

[24] The results of the dilution estimates for the four patches are shown in Figure 6. The initial dilution rates varied considerably: the first release had the least dilution over the first 12 hours; the second and third were comparable; and the fourth release had the most, roughly a factor of 5 greater than release 1 for the same point in time.

[25] The slope of the dilution curve in log space shown in Figure 6 can be used to distinguish 3-D spreading, which would be expected at the beginning of the release, from 2-D and 1-D spreading, which would occur as the vertical and lateral boundaries of the domain started to constrain the spreading. The dilution rate for 3-D spreading varies as $t^{-3/2}$ (assuming steady but not isotropic dispersion coefficients); for 2-D spreading it should be t^{-1}, and for 1-D spreading $t^{-1/2}$. Although the assumption of a constant dispersion coefficient is questionable, the general tendency of rapid initial dilution followed by a reduction of the rate is roughly consistent with a decrease in dimensionality of the spreading with time. All of the releases show dilution roughly consistent with 3-d spreading for the first 9–12 hours. For the 2nd and 3rd releases, the dilution rate diminished after 12 hours, becoming roughly consistent with 1-d spreading, although release 3 showed a subsequent increase in dilution around 30 hours that suggests a more complex dilution process.

[26] In order to provide a quantitative sense of the relationship between dilution and spreading of the dye, the ''equivalent volume'' of the dye patch was calculated based on the dilution estimate (note right axis of Figure 6). The calculation of volume was based on the assumption that the concentrations were normally distributed, with the volume including all of the fluid with concentrations greater than 5% of the maximum value. The ''equivalent volume'' could thus be considered the volume of an ellipsoid of dye

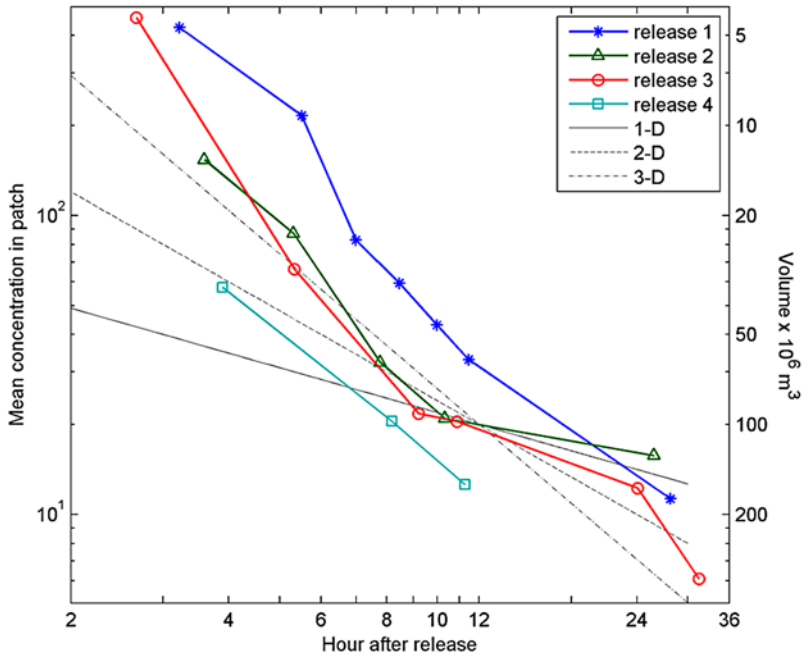

Figure 6. Patch-averaged dye concentration (units 10^{-8} kg/m^3; left axis) for all 4 releases as a function of time since the release. The equivalent volume of the patch is shown on the right. Also shown are lines of constant dilution rate for 1-dimensional, 2-dimensional and 3-dimensional spreading.

with the same mass and mean concentration as the observations. Although not exact, it provides a convenient means of converting the observed concentration to a volume. The first observations of the patch volume (3–4 hours after release) were on the order of 5×10^6 m^3, and after 12 hours the patch had expanded to $50–200 \times 10^6$ m^3.

[27] The volume of the patch during the 4th release was 4–5 times the volume on the 1st release, indicating the much greater mixing during the spring-tide conditions of the 4th release. The vertical and lateral distributions of dye were resolved in fine detail by the shipboard sampling program (0.2 m and 50-m, respectively), but the along-estuary distributions were often relatively coarse (e.g., Figure 2). Gaussian fits to the along-estuary data (as discussed in section 2) reduced the sensitivity of the estimate of spreading rate to the distribution of data. The Gaussian fits for the first release are shown in Figure 7. Most of the data are well represented by the Gaussian, and in most cases the regression coefficient r^2 exceeds 0.9. The Gaussian fit generally yielded a slightly larger estimate of the variance (10–20%) than the direct calculation. This is because the tails of the distribution were not fully resolved. A Gaussian fit was not appropriate for the vertical or lateral distributions, because the stratification and/or bathymetry caused the distributions to be non-Gaussian (e.g., Figures 3 and 4).

3.2.1. Vertical Spreading

[28] The time-evolution of the moments of the dye distribution are shown in Figure 8. The equivalent physical dimensions of the patch are shown along the right axis. There was a clear indication of the dependence of spreading rate on the stage of the spring-neap cycle: the most strongly stratified, neap tide conditions (release 1) show nearly an order of magnitude lower mean vertical mixing rate than the weakly stratified, strong spring-tide (release 4). The other two are intermediate in vertical spreading. The "effective" vertical diffusivities were estimated from equation (7), and surprisingly small numbers were obtained. The average vertical spreading rate for the neap tide (over 25 hours) was 4×10^{-5} m^2 s^{-1}, and for spring tides it averaged 2×10^{-4} m^2 s^{-1}. This number does not represent the vertically averaged diffusivity; it is actually closer to an estimate of the minimum diffusivity in the pycnocline, as the dye spreads to fill the mixed layer, but its vertical spreading is limited by the minimum in K_z in the pycnocline [e.g., *Chant et al.*, 2007]. Still, this estimate of K_z can yield an approximate timescale for vertical mixing, which can be determined as

$$T_z = h^2/10K_z \tag{8}$$

[*Fischer et al.*, 1979], yielding mixing timescales of 16 hours for spring tides and 6 days for neap tides (based on an average depth of 12 m). In both cases they considerably exceed the tidal timescale, and in the case of neap mixing the timescale is on the same order as the neap-to-spring transition. These observations occurred during a period of significant freshwater flow and relatively strong stratification (Table 1), and more rapid mixing would be expected during weaker stratification conditions.

[29] Tidal variations in mixing were not well resolved by the vertical spreading rate; there was no indication of reduced mixing during ebb relative to flood as expected due to tidal straining. This could be explained in that straining only affects the mixing within the boundary layer [*Stacey and Ralston*, 2005], and the mixing above the

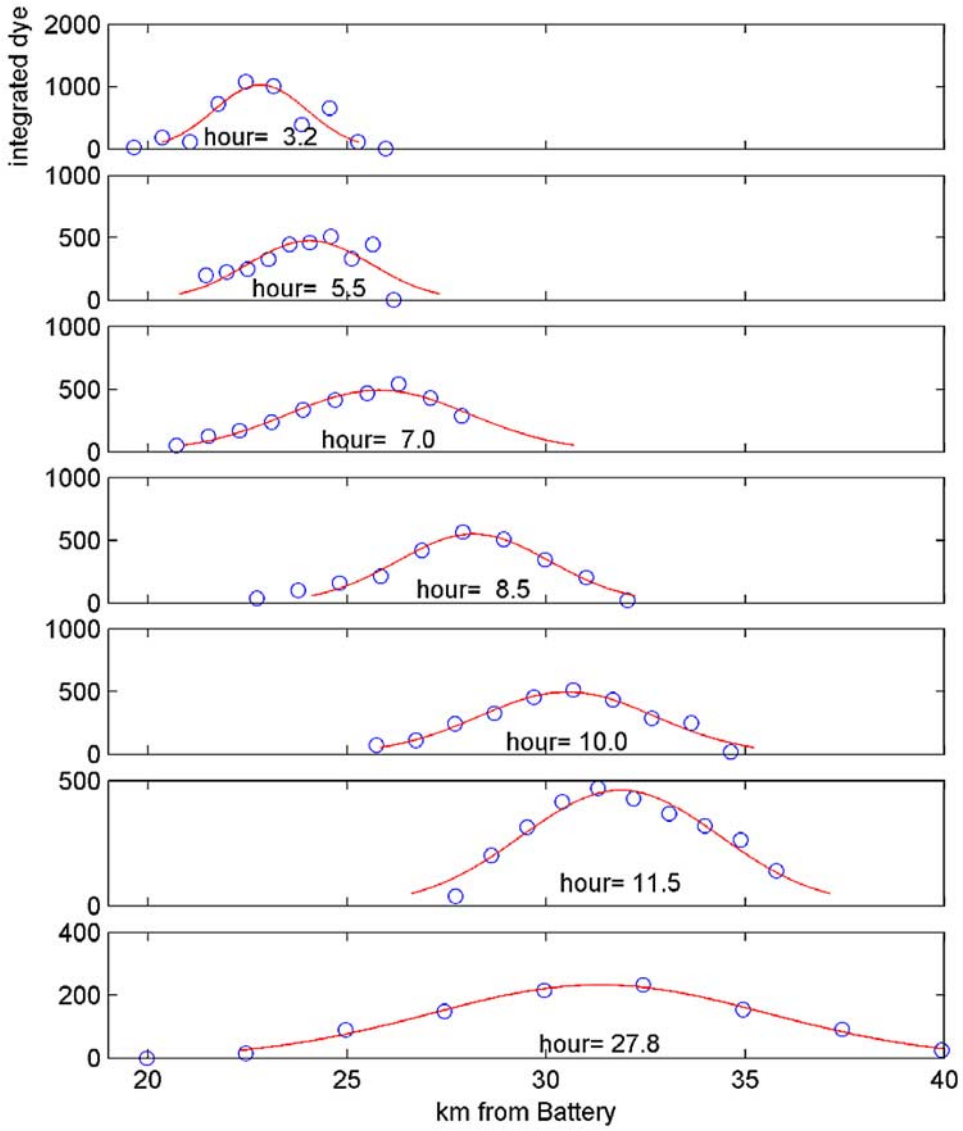

Figure 7. Gaussian fits to the along-channel distribution of the vertically integrated, laterally averaged concentration (units 10^{-8} kg/m^2) during the first release.

boundary layer during the flood tide (e.g., Figure 3) was strongly attenuated by stratification. The occasional observations of reduction of the vertical moment (e.g., Release 3 between hour 5 and 9 in Figure 8, upper panel) suggest the imprecision of this method for estimating vertical mixing. The reduction is probably due to lateral and/or longitudinal extension of the patch that caused a reduction of the vertical moment that exceeded the increase due to mixing.

3.2.2. Cross-Estuary Spreading

[30] The initial lateral mixing was quite rapid (relative to the scale of the channel width) for all of the releases (Figure 8, 2nd panel). The timescale of lateral mixing is estimated as

$$T_x = W^2/10K_x \tag{9}$$

[*Fischer et al.*, 1979], yielding lateral mixing timescales of 1/2 d to 1.5 d based on the initial spreading rates. The timescale for lateral mixing is considerably faster than vertical mixing during the neaps, and comparable during the springs. The spreading rate slowed down after the 1st tidal cycle in all cases, due mainly to the geometric constraint of the channel (see Figure 4).

[31] One notable aspect of the lateral spreading is the contrast in initial spreading rates of the 2nd and 4th releases, which were initiated during the floods, relative to releases 1 and 3, which occurred during the ebbs. This difference is consistent with the model result of *Lerczak and Geyer* [2004] of much stronger transverse circulation during flood than ebb, which drives the lateral shear dispersion in an estuary. The higher lateral spreading during the floods would also be augmented by the thicker boundary layer during flood, which would increase the effectiveness of lateral shear dispersion (discussed below).

[32] The comparison of spring versus neap tide releases did not indicate significant dependence of initial lateral spreading on the tidal amplitude. The first release (weak

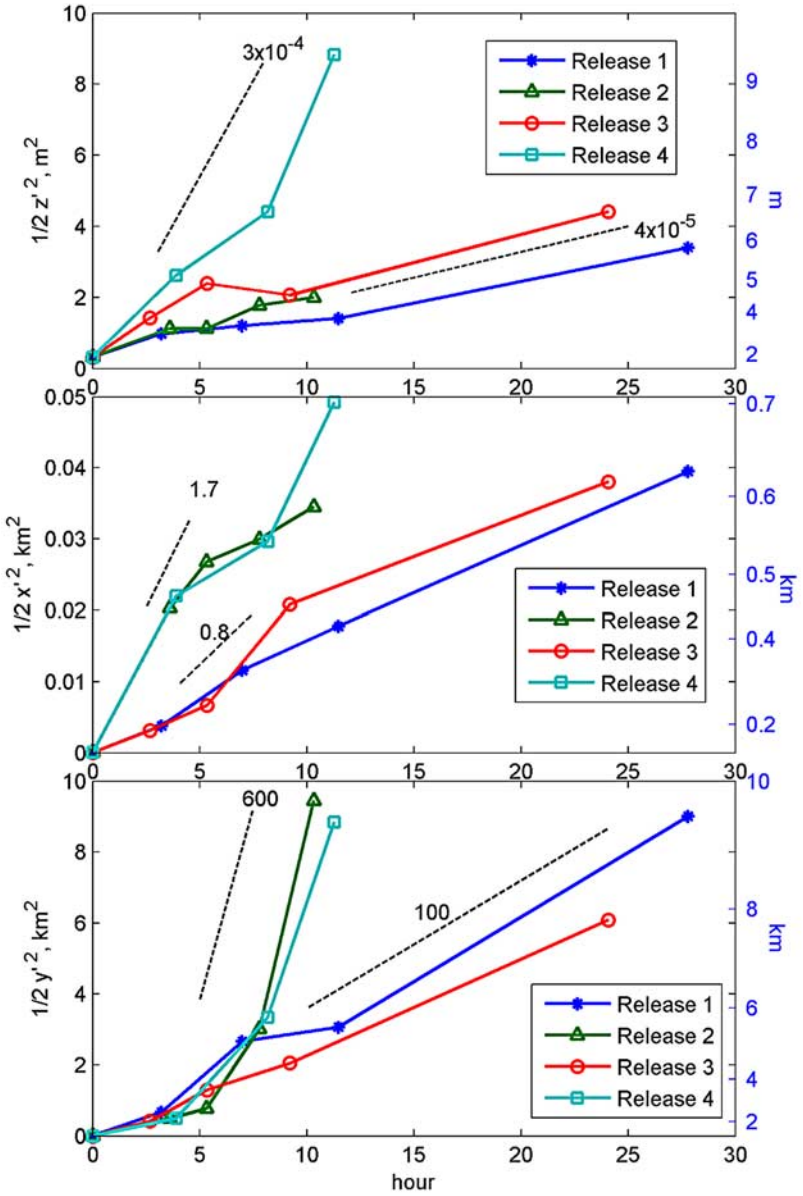

Figure 8. Time evolution of the 2nd moment of the dye distribution in the vertical (top), cross-estuary (middle), and along-estuary (bottom). Dashed lines indicate values of dispersion rate (m^2/s) for different slopes. The right-hand axis indicates the equivalent length scale of the patch ($\sim 4\ x'$).

neap tides) did show less lateral spreading than the other releases. This may be attributed to the more limited vertical scale of the patch, which leads to more of a lateral bathymetric constraint on spreading.

3.2.3. Along-Estuary Spreading

[33] The along-estuary spreading rate (or the longitudinal dispersion) indicated significant short-term variability (Figure 8, lower panel). Because the releases occurred during different tidal phase, it is difficult to discern from this figure the tidal dependence of dispersion. Estimates of dispersion rate (based on the slopes of the segments in Figure 8) are plotted as a function of tidal phase in Figure 9, showing the tidal variability of the dispersion rate. The maximum along-estuary dispersion was observed at the end of the ebb during the 2nd and 4th releases, with a rate reaching 500–700 m^2/s. The period of rapid spreading corresponds to the times of the observations shown in Figure 5, when there was pronounced vertical shearing of the patch during both the 2nd and 4th release. The ebb shears had less influence on the 1st and 3rd releases, apparently because the dye patch was too close to the bottom during the ebb just following the release for significant dispersion to occur. (The influence of the vertical extent of the patch on spreading is examined in more detail in the Discussion.)

[34] The along-estuary spreading during the flood was weak for all of the releases. The average dispersion rate during the flood was determined to be in the range 20–40 m^2/s. There were also intervals of negative dispersion over

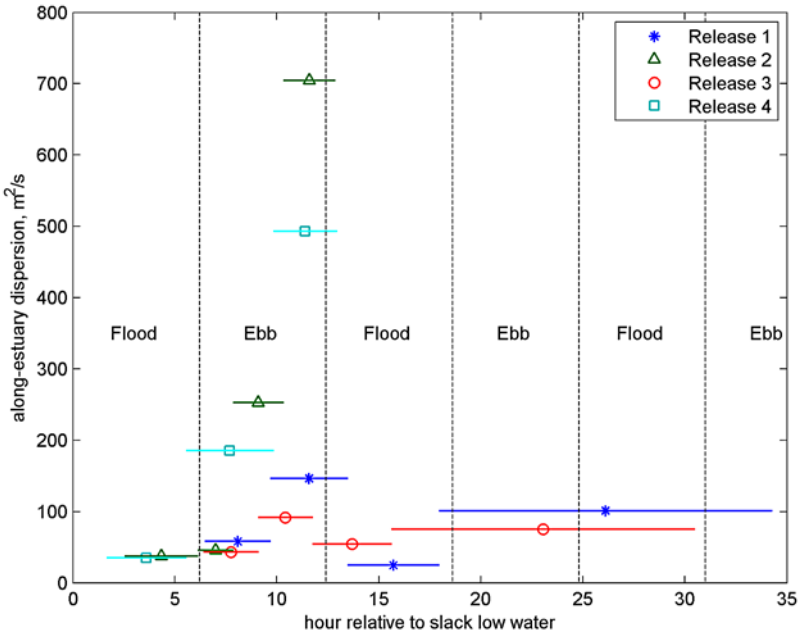

Figure 9. Estimated along-estuary dispersion rate (m^2/s) for the segments shown in Figure 8 (bottom) as a function of tidal phase (referenced to low slack). The horizontal lines indicate the beginning and end of the interval over which the dispersion rate is estimated. Note that not all of the surveys are included, as the estimates between closely spaced surveys were highly variable.

short intervals during the flood (not shown in Figure 8 and 9), in which the patch actually reduced in along-estuary extent. This may have been due in part to incomplete sampling of the patch, but it may have also been caused by an increase in channel cross-section or a reversal of straining (discussed below).

[35] Tidal average dispersion rates could be determined for releases 1 and 3, based on observations on successive days. These indicate tidally averaged dispersion rates of 80–100 m^2/s. Note that the sampling regime did not provide resolution of the second ebb (in the middle of the night), but it would be expected that similarly high dispersion rates would have occurred then.

4. Discussion

[36] The initial dilution of the dye was influenced by spreading in all three dimensions. Only after the first tidal cycle did the lateral constraints of the bathymetry limit lateral spreading. Given enough time, the vertical scale of the patch would likewise be limited by the total depth. The strong vertical stratification inhibited vertical mixing enough during the first 3 releases to prevent the vertical homogenization. The 4th release was headed toward vertical homogenization during the 1st tidal cycle, but the patch was too dilute by the 2nd day to achieve reliable measurements. The estimated timescale of vertical mixing indicates that the transition to one-dimensional, along-estuary spreading should occur in about 1 d for spring tide conditions and 6 d for neap-tide conditions. The limited vertical mixing during neaps significantly limits the dilution, and it also has important consequences for longitudinal spreading, as discussed below. In the remainder of the discussion, the magnitudes and mechanisms of mixing and dispersion in the three dimensions are discussed, to put the observed rates into context with the estuarine regime and with expectations for other systems.

4.1. Vertical Diffusivity

[37] The estimated vertical diffusivities of 4×10^{-5} m^2 s^{-1} and 3×10^{-4} m^2 s^{-1} for neap and spring tides, respectively, are on the low end of the range of estimates by other investigators in the Hudson River. *Peters and Bokhorst* [2001] used a microstructure profiler to estimate much higher diffusivities of $1–5 \times 10^{-2}$ m^2 s^{-1} in the bottom mixed layer. However, they found a minimum diffusivity of 1×10^{-5} m^2 s^{-1} in the pycnocline. *Chant et al.* [2007] found maximum values for diffusivity of $1–5 \times 10^{-3}$ m^2 s^{-1} for neap tides and transition from neap to spring within the bottom mixed layer, based on analysis of the vertical structure of the dye measurements presented here. This comparison suggests that the vertical spreading of dye estimated here is representative of the mixing rates at the top of the dye patch, not the average over the bottom mixed layer. The strong mixing within the bottom mixed layer influences the initial spreading of the dye, but at timescales longer than several hours the reduced mixing in the pycnocline determines the rate.

[38] The strength of the shear and stratification within the pycnocline were estimated for each of the releases, based on the density profiles and velocity from the shipboard ADCP (Table 3). The stratification was strongest during the first two cruises and weakest during the spring tide. Shears also decreased, and most importantly, the gradient Richardson number decreased from a stable value of 0.7 on the 1st two cruises to near its critical value of 0.25 during the fourth cruise. The increase in mixing during the final cruise is

Table 3. Factors Influencing Intensity of Vertical Mixing Buoyancy Frequency N, Shear, and Ri are Based on Measurements[a]

	N s^{-1}	Shear s^{-1}	Ri	K_z m^2 s^{-1}
Release 1	0.13	0.15	0.7	3×10^{-5}
Release 2	0.14	0.16	0.7	3×10^{-5}
Release 3	0.09	0.12	0.5	5×10^{-5}
Release 4	0.05	0.10	0.24	2×10^{-4} [b]

[a]Kz is based on dye moments.
[b]Elapsed time 8 hours.

consistent with this change in the stability of the stratified shear flow.

4.2. Along-Estuary Dispersion

4.2.1. Vertical Shear Dispersion

[39] The along-estuary dispersion of the dye appears to be due to vertical shear dispersion, based on the rapid spreading during the ebb and the distortion of the patch due the vertical shear (Figure 5). The observed rates of along-estuary shear dispersion were compared with Taylor's steady shear dispersion theory equation (1) and (2). The estimate of the nondimensional coefficient α equation (2) depends on the shape of the velocity and diffusivity profiles; a linear profile was chosen for velocity (cf. Figure 5), and the diffusivity was assumed to be constant across the dye patch. This is a crude approximation, but it is adequate for the order-of-magnitude estimates being performed here. For these simple profiles, $\alpha = 8 \times 10^{-3}$. This value of α is considerably larger than its value for unstratified boundary layers [typically $1-2 \times 10^{-3}$, based on *Bowden*, 1965], due to the constant shear extending through the mixing layer, in contrast to a log layer in which most of the shear is confined to a thin near-bottom layer.

[40] Three cases are considered: the flooding tide of the 1st release (Figure 3), the ebb of the 2nd release (Figure 5a), and the ebb of the 4th release (Figure 5b). For the flood tide case, the vertical spreading rate of the dye does not provide a relevant estimate of K_z, because it greatly underestimates the mixing rate in the weakly stratified boundary layer. For the same data set, *Chant et al.* [2007] used an entrainment model to estimate the boundary layer mixing rate at $1-2 \times 10^{-3}$ m^2/s. The vertical velocity difference for the flood was approximately 0.5 m/s, and the layer thickness was 3–4 m. This leads to an estimated horizontal dispersion rate K_y of 9–32 m^2/s. This value is consistent with the crude estimate of the flood-tide dispersion of 20 m^2/s. The time-scale for vertical mixing within the boundary layer for these conditions (equation 8) is 10–30 minutes—much less than the tidal timescale, so the steady shear dispersion model is valid in this case.

[41] For the ebb data, the vertical spreading of the dye patch provides a more reliable estimate of the vertical mixing rate, because the vertical mixing rate is expected to be more uniform through the water column during the ebb [*Peters and Bokhorst*, 2000; *Geyer et al.*, 2000]. Also, the entrainment model of *Chant et al.* [2007] was not applicable to the more vertically continuous vertical gradients observed during the ebb. For release 2, the estimate of vertical mixing rate is roughly estimated at $K_z = 4 \times 10^{-5}$ m^2/s, based the slope of the vertical spreading curve between 5 and 10 hours (Figure 8a). The velocity range across the boundary layer was 0.8 m/s, and the patch thickness was estimated at 5-m (note that the apparent patch thickness in Figure 5 is greater than the patch-average, as the section is in the thalweg). Based on these values and $\alpha = 8 \times 10^{-3}$, equation (1) yields a value for the along-estuary dispersion rate K_y = 3000 m^2/s. This estimate is a factor of 5 greater than the dispersion rate estimated from spreading (Figures 8 and 9) which reaches a maximum of 700 m^2/s. Before addressing the failure of this estimation of shear dispersion, we consider the spring-tide case.

[42] The vertical mixing rate was increasing rapidly during Release 4, but a rough estimate of $K_z = 5 \times 10^{-4}$ m^2/s is appropriate for the period of rapid horizontal spreading (8–11 hours). The velocity difference across the layer was much weaker than Release 2, approximately 0.3 m/s (Figure 5), and the patch thickness was about 9 m. Using the same value for α, the estimated dispersion rate dispersion rate K_y = 120 m^2/s. This estimate is a factor of 5 *lower* than the observed rate of about 500 m^2/s (Figures 8 and 9). The smaller vertical shears and larger mixing rate during Release 4 significantly reduce the vertical shear dispersion rate. Yet the observed dispersion is considerably higher in this case. What explains these discrepancies from the steady vertical shear-dispersion model?

4.2.2. Time-Dependent, "Reversible" Straining

[43] The highly skewed dye distribution in Figure 5 provides key evidence that during the ebb in neap-tide conditions, the vertical mixing does not keep pace with the straining of the patch. In other words, the vertical mixing time-scale significantly exceeds the time-scale over which the strain is acting, in this case roughly 3 hours of maximum ebb shear. On the basis of equation (8), the mixing timescale for a 5-m thick patch with $K_z = 0.4 \times 10^{-4}$ m^2/s is 17 hours, indicating a violation of the quasi-steady assumption of the shear dispersion model. For the spring-tide case, the mixing timescale for a 9-m thick patch with $K_z = 5 \times 10^{-4}$ m^2/s is 4.5 hours, the same order as the tidal forcing and consistent with the quasi-steady assumption.

[44] For the neap-tide regime, a more appropriate model of the "dispersion" process (really a reversible straining process) is to consider the change in horizontal moment of a patch that is strained by a shear flow with no mixing. The effective "dispersion rate" can be derived by considering a slab that is initially rectangular, but is deformed by a uniform shear of magnitude $\Delta u/h$ (where Δu is the velocity difference across the slab and h is its height). The horizontal second moment of the slab is found to be

$$x'^2 = x_o'^2 + \frac{1}{12}(\Delta u)^2 t^2 \tag{10}$$

where $x_o'^2$ is the moment of the initial slab, and the 2nd term is the contribution of the shearing to the 2nd moment. Using the definition of the horizontal dispersion coefficient equation (7), the effective "dispersion rate" for a constant shear across the patch is simply

$$K_s = \frac{1}{2}\frac{d}{dt}x'^2 = \frac{1}{12}(\Delta u)^2 t \tag{11}$$

where the subscript s refers to the straining process, Δu is the velocity difference across the patch, and t is the time

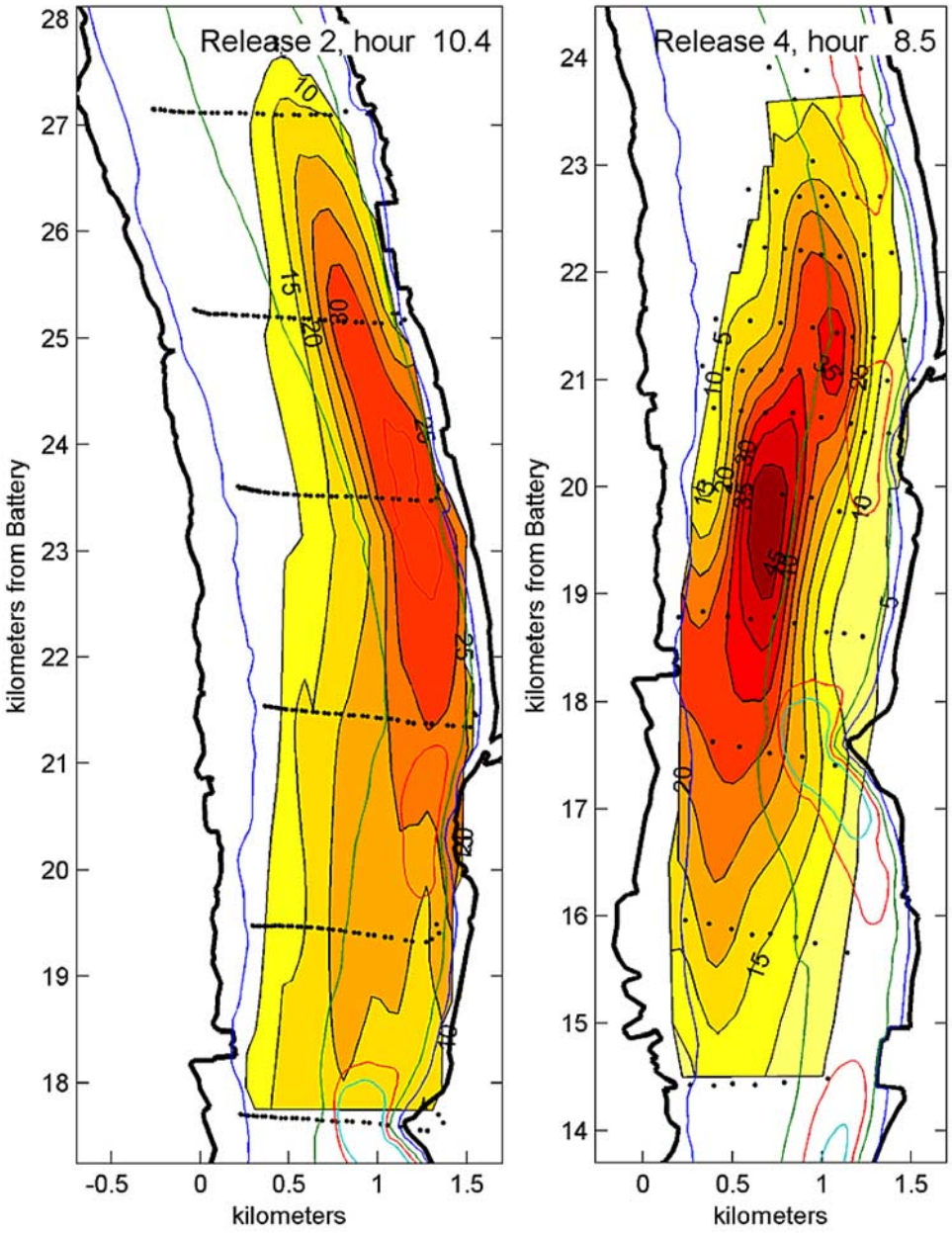

Figure 10. Contours of vertically averaged dye concentration for mid to late ebb conditions during release 2 (left) and release 4 (right). The dye contours approximately follow the bathymetry during the release 2 ebb, whereas the patch is tilted across the estuary during release 4. This provides an indication of the varying role of lateral shear dispersion.

interval over which the shear has acted. For timescales significantly less than the mixing time-scale, equation (11) is applicable, and for longer timescales, equation (1) applies.

[45] For the neap-tide, ebb straining case, the "effective" dispersion coefficient using equation (11) with a 3-hour period of vertical shear with Δu = 0.8 m/s is 580 m^2/s, much closer to the observation of 700 m^2/s. The mixing timescale of 17 hours would suggest that this straining is reversible with the change of shear between flood and ebb. This reversal may partially explain the apparent negative dispersion rates observed in some instances (Figure 8, bottom panel). The vertical mixing rate does increase during the flood tide, and lateral exchange also contributes to the irreversible distortion of the patch, so as to "lock in" its along-estuary extension and thus contribute to the net dispersion.

4.2.3. Lateral Shear Dispersion

[46] The dispersion during spring-tide conditions was much greater than the prediction of the steady shear-dispersion model; this discrepancy appears to be most readily explained by the contribution of lateral shear dispersion. Plan views of the dye distributions of releases 2 and 4 during the ebb spreading phase (Figure 10) show that there was a distinct cross-estuary shearing of the patch during release 4, which is caused by higher southward velocities on

Table 4. Estimates of Shear Dispersion Rate Based on Tidally Averaged Conditions[a]

Release	$\bar{u}_{bl}$	h_{bl}	$K_{z\ (Chant\ et\ al.)}$	$K_{x\ (equation\ (1))}$	$K_{x\ (observed)}$
1	0.29 m/s	6 m	1×10^{-3} m^2/s	25 m^2/s	100 m^2/s
3	0.15 m/s	7 m	2×10^{-3} m^2/s	4 m^2/s	70 m^2/s

[a] $\bar{u}_{bl}$ is the tidally averaged velocity in the boundary layer, h_{bl} is the boundary layer height, $K_{z\ (Chant\ et\ al.)}$ is the estimated vertical mixing rate in the boundary layer from *Chant et al.* [2007], $K_{x\ (equation\ (1))}$ is the estimated dispersion rate based on applying equation (1) to these tidally averaged quantities, and $K_{x\ (observed)}$ is the observed dispersion rate over a tidal cycle (from Figure 8).

the west side (as measured by the moored array, as well as shipboard ADCP data). In contrast, the dye patch during release 2 essentially follows the topography, with only slight influence of distortion by the transverse shear. The difference in the lateral straining of the patch between these two releases is due in part to more transverse shear during the spring-tide conditions; it is also due to the greater vertical extent of the patch during release 4, allowing the patch to extend onto the shallower west flank and into the stronger ebb flow.

[47] The equation for lateral shear dispersion is analogous to equation (1), with h replaced with the width W of the patch, and K_z replaced with K_x, which is obtained directly from the analysis of lateral spreading. In this case u corresponds to the transverse velocity difference across the patch. For the ebb period of release 4, the lateral velocity difference was estimated at 0.5 m/s, based on the moored ADCPs in the cross-estuary array (Figure 1). The width of the patch is estimated at 600 m (from Figure 8), and the transverse diffusion rate ranged from 0.4 to 1.7 m^2/s (also from Figure 8). The transverse diffusivity and shear were assumed to be constant, again yielding a value of $\alpha = 8 \times 10^{-3}$. The resulting estimate for K_h is 400–1800 m^2/s, with the uncertainty resulting from the range of estimates of lateral diffusion rate. The observed along-estuary spreading rate of 600 m^2/s (Figure 8b) is within the range of these estimates, more consistent with the value corresponding to the higher lateral diffusion rate.

[48] Again the applicability of the steady state approximation should be considered: the timescale of transverse mixing based on those two estimates of transverse diffusion are 25 and 6 hours, respectively. The timescale of the lateral shear is 6 hours at most, so the steady shear-dispersion model would not apply for the low value of lateral diffusion. So at the beginning of the ebb, the lateral distortion of the patch occurred as reversible straining, but later in the ebb the intensified lateral mixing resulted in irreversible dispersion of the patch.

4.2.4. Tidally Averaged Along-Estuary Dispersion

[49] Finally, we consider the time-averaged longitudinal dispersion of the releases, which ranged from 70 to 100 m^2/s for the 1st 3 releases (with inadequate data to determine the 4th). We compare these rates to the prediction of the steady shear dispersion theory equation (1), using estimates for the tidally averaged lower layer velocity and layer thickness. The estimated vertical mixing rate in the lower layer is based on *Chant et al.* [2007]. The results of these calculations are shown in Table 4. Note that the observed, tidally averaged dispersion rate is as much as an order of magnitude larger than the value based on the mean conditions.

[50] This calculation suggests, not surprisingly, that the tidally averaged shear dispersion rate is not well represented by the average conditions. It appears that the intense dispersion during the ebb is the main process responsible for the tidally averaged dispersion. The weak dispersion rate during the flood makes a minimal contribution to the tidal average, and the large strain during the ebb contributes virtually all of the net tidal-cycle dispersion. Although the weak mixing rate during the neap ebb tide suggests that the large ebb strain may be reversible, the observed moments only indicate a slight amount of "negative dispersion" during the flood. Vertical mixing during the flood as well as lateral dispersion limit the amount of reversible strain, so most of the ebb-generated strain persists through the tidal cycle.

4.3. Lateral (Cross-Estuary) Dispersion

[51] We have previously discussed the along-estuary dispersion due to lateral variations in the along-channel currents; here we discuss the lateral dispersion due to vertically varying cross-estuary currents. The moored array indicates significant transverse velocity shears in the bottom boundary layer during flood tides [also see *Lerczak and Geyer*, 2004], with velocity differences of 0.1 m/s across the bottom 5-m of the water column. The lateral shear dispersion rate was estimated for these flood-tide conditions based on the Taylor shear dispersion model, again using the Chant et al. values for K_z of $1–2 \times 10^{-3}$ m^2/s, $\alpha = 8 \times 10^{-3}$, and h = 3.5 and 5 m for Releases 2 and 4, respectively. Equation (1) yields estimates of $K_x \cong 1$ m^2/s for the two cases, not too different from the observed lateral spreading (Figure 8) of 1.7 m^2/s for releases 2 and 4. The difference of a factor of 2 is well within the uncertainty of the transverse shear and mixing rates.

[52] The lateral velocity differences were much smaller during the ebbs, on the order of 0.01–0.04 m/s, yielding lateral diffusivities of 0.2 m^2/s or less, consistent with the observations of the initial spreading during Releases 1 and 3. Thus to within the precision of the estimates, the magnitude as well as the tidal phase dependence of the observed lateral dispersion are consistent with the Taylor shear dispersion model.

4.4. Comparison With Estimates of Overall Estuarine Dispersion

[53] *Lerczak et al.* [2006] performed a detailed analysis of the salt flux for the Hudson estuary based on the moored array deployed during the dye study. They estimated the effective longitudinal dispersion rate for the estuary based on the global salt balance equation (3), averaging over tides and low-frequency oscillations. On the basis of the Lerczak et al. calculation of the time series of the along-estuary dispersion coefficient, its value is estimated at 900, 1000, 1500, and 300 m^2/s for the times corresponding to the 4 dye

releases. Only during the 4th release is there any consistency between these estimates and those derived by the spreading of the dye; during the 1st 3 releases there is roughly an order of magnitude discrepancy. What would explain this difference?

[54] The magnitude of horizontal dispersion in a shear flow is very sensitive to the vertical extent of the dye. If one considers a constant shear (a reasonable approximation for the Hudson observations), the velocity scale across the patch is linearly related to the height h of the patch. Thus from equation (1) the horizontal dispersion coefficient depends on h^4, assuming a constant value for K_z. In the first 3 releases, the dye patch filled roughly half the water column during the observed spreading. Increasing h by a factor of 2 would increase the estimate of K_h by a factor of 16, providing the order of magnitude adjustment that is required. This is somewhat of an oversimplification, the velocity profile is not exactly linear, and the vertical diffusivity is not constant, but the extreme sensitivity of dispersion to the vertical extent of the patch provides the main explanation for the apparently small dispersion estimates.

5. Conclusions and Implications

[55] This study revealed very strong temporal and spatial variations in mixing intensity in the Hudson River, indicating the strong stabilizing influence of stratification even in a strongly forced estuarine flow. The timescale for complete vertical mixing is as long as 6 days during neap tides, with the implication that the dye was confined to the lower half of the water column during three of the four releases. When vertical mixing was strong enough to satisfy the quasi-steady approximation, the along-estuary and lateral spreading of the dye were well characterized by the simple shear dispersion model of *Taylor* [1954]. For the neap, ebb conditions, the quasi-steady approximation was invalid, and the spreading of dye was characterized by reversible, time-dependent strain. However, there was minimal reversal of strain, due to mixing and lateral dispersion. In most cases vertical shear dispersion was the dominant mechanism responsible for spreading. Only during spring tides, when the dye extended through most of the water column, did lateral shears become significant in the dispersion process. During these spring-tide conditions, the vertical mixing rate was strong enough to diminish the vertical shear dispersion process. The lateral shear became the most important agent elongating the patch, but lateral mixing was not fast enough to yield a steady state balance, so time-dependent straining rather that shear dispersion explains the along-estuary spreading rate during those conditions.

[56] Tidal straining was found to have a strong influence on the tidal variations of longitudinal dispersion. The weak vertical mixing and strong shears during the ebb caused virtually all of the longitudinal dispersion to occur during the ebb tide. The lateral dispersion also showed strong tidal variability, with its maximum occurring during the flood tide due to stronger transverse shears (i.e., secondary circulations) during the flood than the ebb. This is consistent with model results of *Lerczak and Geyer* [2004] of the tidal variability of the secondary circulation in partially mixed estuaries.

[57] A notable finding is the large difference between the dispersion rate of the dye and the overall dispersion rate of the estuary. During the neap-tide releases, the vertical extent of the dye was significantly less than the overall water depth, which reduces the effective dispersion rate as roughly the 4th power of the fractional depth of the dye (assuming linear shear). If the initial distribution of dye extended through the entire water column, the dispersion rate of dye would be the same as the overall estuarine dispersion rate, which reaches the extraordinary rate of more than 2000 m^2/s during neap tides according to *Lerczak et al.* [2006]. Such large dispersion rates require very weak levels of vertical mixing across the pycnocline, consistent with these observations of $K_z = 4 \times 10^{-5}$ m^2/s in the pycnocline during the neaps. However, the weak mixing rates result in long vertical adjustment timescales, so the large value of shear dispersion is only applicable to substances (such as salt) that have been in the estuary long enough to be broadly distributed in the vertical. During spring tides, the dye makes it to the surface within 1–2 tidal cycles, but vertical shear dispersion is reduced by the higher vertical mixing rates. Lateral shear dispersion during spring tides is significant, but it does not reach comparable magnitudes of the vertical shear dispersion during neaps.

[58] **Acknowledgments.** The authors would like to acknowledge Jim Lerczak for his logistical and intellectual contributions to this effort. Jay Sisson orchestrated the field work, and Eli Hunter contributed to the data analysis. This research was supported by National Science Foundation Grant OCE04-52054 (W. Geyer), OCE00-99310 (R. Houghton), and OCE00-95913 (R. Chant).

References

Banas, N. S., B. M. Hickey, and P. MacCready (2004), Dynamics of Willapa Bay, Washington: A highly unsteady, partially mixed estuary, *J. Phys. Oceanogr.*, *34*, 2413–2427.

Bowden, K. F. (1965), Horizontal mixing in the sea due to a shearing current, *J. Fluid Mech.*, *21*, 83–95.

Bowen, M. M., and W. R. Geyer (2003), Salt transport and the time-dependent salt balance of a partially stratified estuary, *J. Geophys. Res.*, *108*(C5), 3158, doi:10.1029/2001JC001231.

Chant, R. J., W. R. Geyer, R. Houghton, E. Hunter, and J. A. Lerczak (2007), Bottom boundary layer mixing and the estuarine neap/spring transition, *J. Phys. Oceanogr.*, *37*, 1859–1877.

Clark, J. F., P. Schlosser, M. Stute, and H. J. Simpson (1996), SF_6– ^3He tracer release experiment: A new method of determining longitudinal dispersion coefficients in large rivers, *Environ. Sci. Technol.*, *30*, 1527–1532.

Cole, J. J., N. F. Caraco, and B. L. Peierls (1992), Can phytoplankton maintain a positive carbon balance in a turbid, freshwater, tidal estuary?, *Limnol. Oceanogr.*, *37*, 1608–1617.

Fischer, H. B. (1972), Mass transport mechanisms in partially stratified estuaries, *J. Fluid Mech.*, *53*, 671–687.

Fischer, H. B., E. J. List, R. C. Y. Kho, J. Imberger, and N. H. Brooks (1979), *Mixing in Inland and Coastal Waters*, 483 pp., Elsevier, New York.

Geyer, W. R., and D. M. Farmer (1989), Tide induced variation of the dynamics of a salt wedge estuary, *J. Phys. Oceanogr.*, *28*, 1060–1072.

Geyer, W. R., J. H. Trowbridge, and M. Bowen (2000), The dynamics of a partially mixed estuary, *J. Phys. Oceanogr.*, *30*, 2035–2048.

Guymer, I., and J. R. West (1988), The determination of estuarine diffusion coefficients using a fluorimetric dye tracing technique, *Estuarine Coastal Shelf Sci.*, *27*, 297–310.

Jay, D. A., and J. D. Smith (1990), Circulation, density distribution and neap-spring transitions in the Columbia River Estuary, *Prog. Oceanogr.*, *25*, 81–112.

Ledwell, J. R., A. J. Watson, and C. S. Law (1993), Evidence for slow mixing cross the pycnocline from an open-ocean tracer-release experiment, *Nature*, *364*, 701–703.

Lerczak, J. A., and W. R. Geyer (2004), Modeling the lateral circulation in straight, stratified estuaries, *J. Phys. Oceanogr.*, *34*, 1410–1428.

Lerczak, J. A., W. R. Geyer, and R. J. Chant (2006), Mechanisms driving the time-dependent salt flux in a partially stratified estuary, *J. Phys. Oceanogr.*, *36*, 2296–2311.

Monismith, S. G., W. Kimmerer, J. R. Burau, and M. T. Stacey (2002), Structure and flow-induced variability of the subtidal salinity field in northern San Francisco Bay, *J. Phys. Oceanogr.*, *32*, 3003–3019.

Okubo, A. (1973), Effects of shoreline irregularities on streamwise dispersion in estuaries and other embayments, *Neth. J. Sea Res.*, *8*, 213–224.

Peters, H., and R. Bokhorst (2000), Microstructure observations of turbulent mixing in a partially mixed estuary. part I: Dissipation rate, *J. Phys. Oceanogr.*, *30*, 1232–1244.

Peters, H., and R. Bokhorst (2001), Microstructure observations of turbulent mixing in a partially mixed estuary. part II: Salt flux and stress, *J. Phys. Oceanogr.*, *31*, 1105–1119.

Simpson, J. H., J. Brown, J. Matthews, and G. Allen (1990), Tidal straining, density currents, and stirring in the control of Estuarine stratification, *Estuaries*, *13*, 125–132.

Smart, P. L., and I. M. S. Laidlaw (1977), An evaluation of some fluorescent dyes for water tracing, *Water Resour. Res.*, *13*, 15–33.

Smith, R. (1977), Long-term dispersion of contaminants in small estuaries, *J. Fluid Mech.*, *82*, 129–146.

Stacey, M. T., and D. K. Ralston (2005), The scaling and structure of the estuarine bottom boundary layer, *J. Phys. Oceanogr.*, *35*, 55–71.

Sumer, S. M., and H. B. Fischer (1977), Transverse mixing in partially stratified flow, *J. Hydraul. Eng., ASCE*, *103*, 587–600.

Taylor, G. (1954), The dispersion of matter in turbulent flow through a pipe, *J. Phys. A, J. Phys. B, J. Phys. C*, *223*, 446–468.

Tyler, M. A. (1984), Dye tracing of a subsurface chlorophyll maximum of a red-tide dinoflagellate to surface frontal regions, *Mar. Biol.*, *78*(3), 265–330.

Vallino, J. J., and C. S. Hopkinson Jr. (1998), Estimation of dispersion and characteristic mixing times in Plum Island Sound estuary, *Estuarine Coastal Shelf Sci.*, *46*, 333–350.

Wang, D. P., and D. W. Kravitz (1980), A semi-implicit two-dimensional model of estuarine circulation, *J. Phys. Oceanogr.*, *10*, 441–454.

Wilson, R. E., and A. Okubo (1978), Longitudinal dispersion in a partially mixed estuary, *J. Mar. Res.*, *36*(3), 427–447.

Young, W. R., and P. B. Rhines (1982), Shear-flow dispersion, internal waves and horizontal mixing in the ocean, *J. Phys. Oceanogr.*, *12*, 515–527.

R. Chant, W. R. Geyer, and R. Houghton, Woods Hole Oceanographic Institution, Applied Ocean Physics and Engineering, Mail Stop 11, Woods Hole, MA 02543, USA. (rgeyer@whoi.edu)